Improving Polypropylene Microcellular Foaming Through Blending and the Addition of Nano-Calcium Carbonate

Han-Xiong Huang, Jian-Kang Wang

Center for Polymer Processing Equipment and Intellectualization, College of Industrial Equipment and Control Engineering, South China University of Technology, Guangzhou, People's Republic of China

Received 12 September 2006; accepted 20 February 2007
DOI 10.1002/app.26483
Published online 26 June 2007 in Wiley InterScience (www.interscience.wiley.com).

ABSTRACT: This article reports an attempt to improve polypropylene (PP) microcellular foaming through the blending of PP with high-density polyethylene (HDPE) as a minor component and the incorporation of nano-calcium carbonate (nano-$CaCO_3$) into PP and its blends with HDPE. Three HDPEs were selected to form three blends with a viscosity ratio less than, close to, or greater than unity. Two concentrations of nano-$CaCO_3$, 5 and 20 wt %, were used. The blends and nanocomposites were prepared with a twin-screw extruder. The foaming was carried out by a batch process with supercritical carbon dioxide as a blowing agent. The online shear viscosity during compounding and the dynamic rheological properties of some samples used for foaming were measured. The cell structure of the foams was examined with scanning electron microscopy (SEM), and the morphological parameters of some foams were calculated from SEM micrographs. The rheological properties of samples were used to explain the resulting cell structure. The results showed that the blend with a viscosity ratio close to unity produced a microcellular foam with the minimum mean cell diameter (0.7 μm) and maximum cell density (1.17 $\times$ 10^{11} cells/cm^3) among the three blends. A foamed PP/nano-$CaCO_3$ composite with 5 wt % nano-$CaCO_3$ exhibited the largest cell density (8.4 $\times$ 10^{11} cells/cm^3). © 2007 Wiley Periodicals, Inc. J Appl Polym Sci 106: 505–513, 2007

Key words: blends; foams; morphology; nanocomposites; poly(propylene) (PP)

INTRODUCTION

In the early 1980s, the concept of microcellular foaming was proposed by Suh.[1] A microcellular foam shows a specific structure whose cell diameter is less than 10 μm and whose cell density is larger than 10^9 cells/cm^3. The microcellular foam structure provides higher mechanical strength, such as higher impact strength and toughness, than conventional foaming while reducing material usage. Therefore, there has been considerable interest in studying microcellular foaming technology since the early 1980s.[2] However, the research has been mainly focused on amorphous polymers.

Colton[3] and Colton and Suh[4] first applied microcellular foaming technology to semicrystalline polymers. Research by Doroudiani et al.[5] showed that the crystalline morphology of semicrystalline polymers has a great effect on the solubility and diffusivity of the blowing agent as well as the cellular structure of the microcellular foams prepared in a batch process. It is known that the microcellular foaming of pure semicrystalline polymers such as polypropylene (PP) is very difficult to achieve through a batch process because of the high crystallinity and sizes of the crystallites,[5–7] except through the quenching of the semicrystalline polymers during cooling from the melt to achieve relatively low crystallinity.[5] Research by Doroudiani et al.[6] and Rachtanapun et al.[7,8] showed that microcellular foams are greatly enhanced through the blending of PP and high-density polyethylene (HDPE) with supercritical carbon dioxide (CO_2) as a blowing agent. In their works, CO_2-saturated PP/HDPE blend samples were microcellular-foamed by immersion in a hot glycerin bath.

Recent research by Okamoto and coworkers[9,10] and Taki et al.[11] showed that microcellular foams could be prepared with PP/clay nanocomposites with CO_2 as a blowing agent. These studies revealed that incorporating nanoclay into PP could effectively reduce the cell diameter and increase the cell density of foams. Scanning electron microscopy (SEM) confirmed that the foamed PP/clay nanocomposites had a high cell density of 10^7–10^8 cells/cm^3, a cell diameter in the range of 30–120 μm, and a cell wall thickness of 5–15 μm.[9,10] The visual observations by Taki et al.[11] showed that the nanoclay could improve the cellular morphology by enhancing the nucleation and retarding the growth of bubbles in the early stage of foaming. Very recently, we investigated the effect of the nano-calcium carbonate (nano-$CaCO_3$)

Correspondence to: H.-X. Huang (mmhuang@scut.edu.cn).
Contract grant sponsor: National Natural Science Foundation of China; contract grant number: 20274012.
Contract grant sponsor: Teaching and Research Award Program for Outstanding Young Teachers in Higher Education Institutions of the Ministry of Education, People's Republic of China.

Journal of Applied Polymer Science, Vol. 106, 505–513 (2007)

concentration on the cellular structure and volume expansion of foamed PP/nano-$CaCO_3$ composites.[12] The results showed that a suitable concentration of nano-$CaCO_3$ increased the cell density and volume expansion of foamed nanocomposites.

PP is a very likely substitute for engineering plastics in general-purpose plastics because of its high heat distortion temperature, yield strength, tensile strength, and so on. However, the shortcomings in the impact strength, shrinkage, and weather endurance of PP make its applications in engineering very difficult. Microcellular foaming can extend the applications of PP because of the special properties of microcellular foams. Therefore, the microcellular foaming of PP using CO_2 is a hot topic in polymer processing.

This work was aimed at improving the foamability of PP through the blending PP with HDPEs of different viscosities and through the incorporation of nano-$CaCO_3$ particles into PP and PP/HDPE blends. The PP/HDPE blends and PP/nano-$CaCO_3$ and PP/HDPE/nano-$CaCO_3$ composites were prepared with the melt-blending method with a twin-screw extruder. Then, the as-extruded blends and nanocomposites were used to prepare foams by a batch process in a pressure vessel with supercritical CO_2 as a blowing agent.

EXPERIMENTAL

Materials

The PP used was grade J501 (Sinopec Group Guangzhou Co., Singapore, China) with a melt index of 2.7 g/10 min at 230°C. This PP was a fiber-extrusion-grade resin. Three HDPE grades with different shear viscosities were used: grade 5502 (Chevron Phillips Singapore Chemicals, Ltd., Singapore, China), grade 60550AG (Sinopec Group Lanzhou Co., China), and grade 5218EA (Sinopec Group Dushanzi Co., China). They are denoted HDPE1, HDPE2, and HDPE3, respectively. The first HDPE, with a melt index of 0.35 g/10 min at 190°C, was an extrusion-blow-molding-grade resin. The latter two, with melt indices of 7.2 and 15 g/10 min at 190°C, respectively, were injection-molding resins.

The nano-$CaCO_3$ used was manufactured by Inner Mongolia Mengxi High-Tech Materials Co., Ltd. (China). This nano-$CaCO_3$ was pretreated by the manufacturer. When the nanocomposites were prepared, stearic acid was used as a coupling agent.

Industrial CO_2 with a purity of 99.5% was directly used as a foaming agent.

Sample preparation

Samples of neat PP, PP/HDPE (75/25 w/w) blends, and PP/nano-$CaCO_3$ (95/5 and 80/20 w/w) and PP/HDPE1/nano-$CaCO_3$ (75/20/5 w/w/w) composites were prepared with a modular corotating, intermeshing twin-screw extruder with a screw diameter of 35 mm and a length-to-diameter ratio of 40 : 1. The nano-$CaCO_3$ was dried in a vacuum oven at 90°C for 4 h and then mixed with the coupling agent for about 10 min to facilitate the dispersion of the nanoparticles in the polymer matrix. The concentration of the coupling agent was 1.5 wt % with respect to nano-$CaCO_3$. The PP or PP/HDPE blends and the nano-$CaCO_3$ particles were dry-mixed thoroughly before being fed into the twin-screw extruder. The compounding was carried out at a temperature profile of 160–180–195–195–190–190–190–190–190°C from the hopper to the strand die. The screw speed was set at 100 rpm.

The extruded strands with a diameter of about 2–3 mm were cooled in a water bath and collected.

Foaming apparatus and procedure

The extruded and cooled strands were cut into short rod samples with a length of about 20 mm and then were used for foaming.

A batch process of microcellular foaming was employed in this work. Figure 1 schematically illustrates the experimental apparatus, the pressure vessel of which was designed by us. The foaming procedure can be briefly described as follows. The samples were first placed in the pressure vessel. The vessel was slowly flushed with CO_2 gas, then heated to 120°C within about 0.5 h, and pressurized to a pressure of 15 or 19 MPa, which was called the saturating/foaming pressure in this work. This pressure was kept by the syringe pump. The samples were saturated in the vessel for 22 h at this pressure. Such a long time of dissolving CO_2 in the samples ensured that the samples were completely saturated. After that, the vessel was heated to the foaming temperature (179 or 182°C) within about 20 min. The spillover gas due to the temperature rise was

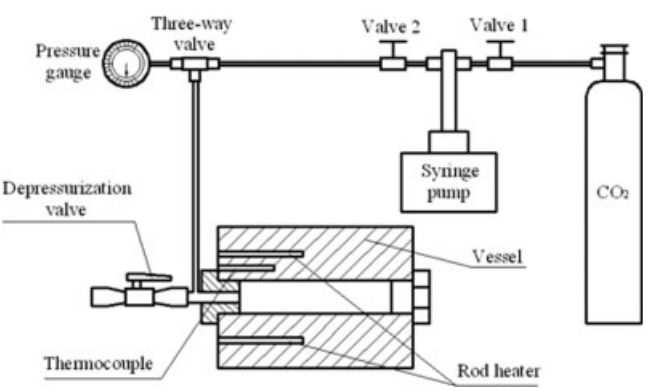

Figure 1 Experimental apparatus for microcellular batch foaming.

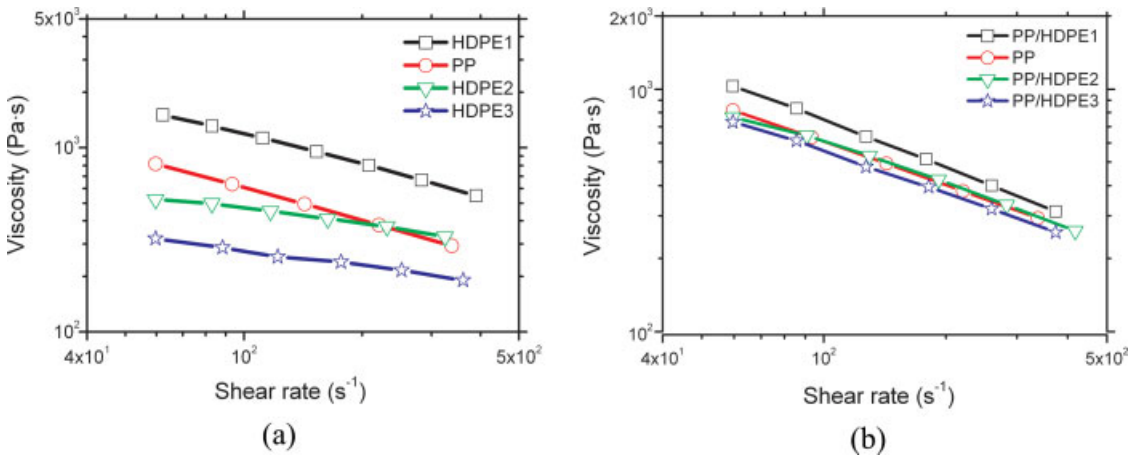

Figure 2 Shear viscosity versus the shear rate for (a) PP and HDPEs and (b) PP/HDPE blends at 190°C. [Color figure can be viewed in the online issue, which is available at www.interscience.wiley.com.]

reclaimed by the syringe pump to keep the pressure in the vessel unchanged. About 1 h later, the vessel was depressurized to the atmospheric pressure in less than 0.5 s by the quick opening of the depressurization valve. A large number of microcells should have been nucleated when the release of the CO_2 pressure started because of the thermodynamic instability. During the subsequent release of CO_2, cells grew to an equilibrium diameter. The foamed samples were injected out of the vessel and cooled in the air.

High-pressure CO_2 was provided by a syringe pump (ISCO 500D) (Teledyne Isco Inc., Lincoln, NE). The vessel was heated with rod heaters. The temperature and pressure were measured with a thermocouple inserted within the wall of vessel and a pressure gauge connected to the vessel cavity, respectively.

Characterization

The melt shear viscosities of pure PP and HDPE and their blends were measured online during the preparation of the samples with a Haake ProFlow online rheometer, which was side-mounted to the end of the twin-screw extruder. The ProFlow system continuously diverted a small flow of material from the end of the twin-screw extruder and pushed that material through a capillary by means of a melt pump. The pressure before the melt pump was controlled by an automatic bypass valve to prevent the disturbance of the process during the measurement.

The dynamic rheological properties of the extruded samples (strands), including the pure PP, PP/HDPE blends, and PP/nano-$CaCO_3$ composites, were measured with a Bohlin Gemini 200 rheometer system (Malvern, Worcetershire, UK) in an oscillatory mode with a parallel-plate geometry and with 25-mm diameter plates at 179°C. The sample was subjected to a cyclic tensile strain with an amplitude of 1% and a frequency range of 0.01–100 s^{-1}.

The foamed sample was immersed in liquid nitrogen for 20 min and then fractured. The fractured surfaces were coated with gold and then examined with a Philips XL-30FEG scanning electron microscope (Holland) at an acceleration voltage of 15 kV to observe the cellular structures of the foamed samples.

To quantitatively assess the SEM micrographs with respect to the cell structures, the SEM gray-level image was converted into a binary image with Scion image software (Beta 4.02, Scion Corp., Frederick, MD), a brightness threshold setting being specified. Through the analysis of the SEM photomicrographs of foamed samples, the mean cell diameter ($\bar{d}$) and cell density (ρ_c) were calculated with the following equations:

$$\bar{d} = \frac{\sum_{i=1}^{n} d_i}{n} \tag{1}$$

$$\rho_c = \left(\frac{NM^2}{A}\right)^{3/2} \tag{2}$$

where d_i is the single cell diameter, n is the number of counted cells, A is the area of the SEM micrograph, N is the number of cells in area A, and M is the magnification factor of the SEM micrograph. About 50 cells in the SEM micrographs for each sample were used to evaluate the mean cell diameter.

The volume expansion ratio (V_r) of the foamed samples was calculated as follows:

$$V_r = \left(\frac{D}{D_0}\right)^3 \tag{3}$$

where D and D_0 are the diameters of the foamed and unfoamed rods, respectively.

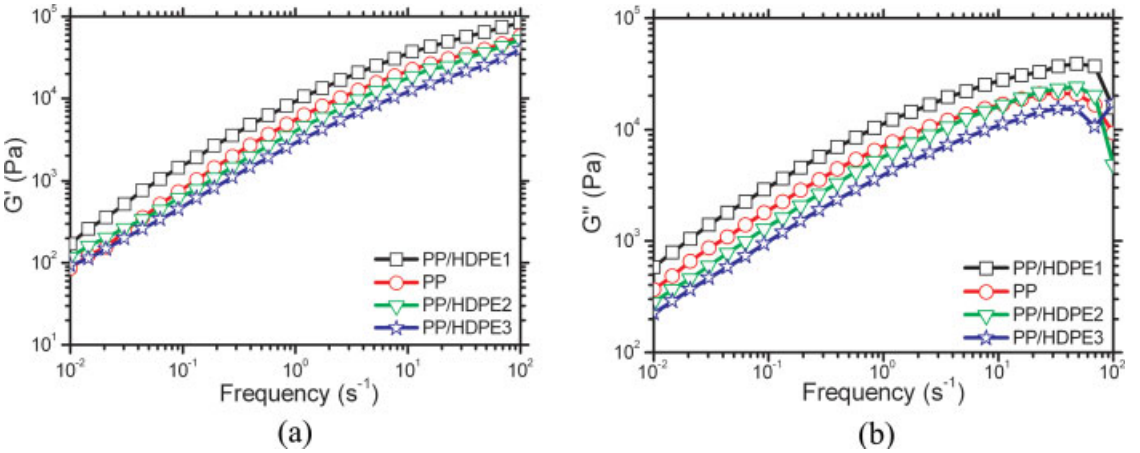

Figure 3 Experimental data for the storage and loss moduli (G' and G'') for PP and PP/HDPE blends at 179°C. [Color figure can be viewed in the online issue, which is available at www.interscience.wiley.com.]

RESULTS AND DISCUSSION

Rheological properties

Figure 2 shows the apparent melt shear viscosity as a function of the shear rate for the pure polymers and three blends at 190°C. As expected, the shear viscosities of the blends decreased with an increase in the melt index of HDPE. It can be calculated from Figure 2 that under 100–400-s^{-1} shear rates, at which the melt experienced when flowing through the kneading block in the twin-screw extruder, the viscosity ratio of the dispersed phase (HDPE) to the matrix (PP) was 2.0–2.1, 0.8–1.3, and 0.5–0.8 for PP/HDPE1, PP/HDPE2, and PP/HDPE3 blends, respectively.

The data on the storage and loss moduli for the PP and three blends obtained at different frequencies are shown in Figure 3. The PP/HDPE1 blend exhibited the highest dynamic moduli. In comparison with pure PP, both the PP/HDPE2 and PP/HDPE3 blends had lower storage moduli over a wide frequency range but higher storage moduli at a very low frequency. Illustrated in Figure 4 is the complex viscosity versus the frequency for the PP and three blends. It is evident that the PP/HDPE1 blend exhibited the highest complex viscosity and that the PP/HDPE2 and PP/HDPE3 blends had lower complex viscosities than pure PP.

The storage and loss moduli of the PP/nano-$CaCO_3$ composites with 5 and 20 wt % nano-$CaCO_3$ and pure PP are shown in Figure 5. Both composites had higher storage moduli than PP at high frequencies, but they had lower storage moduli than PP at low frequencies. Figure 6 illustrates the complex viscosity versus the frequency for PP/nano-$CaCO_3$ composites as well as PP. The composites exhibited higher complex viscosities over a wide frequency range.

Cell structures of the foamed samples

Figure 7 displays the SEM micrographs of foamed PP under different conditions. As can be directly observed, PP could not be foamed at the foaming temperature of 179°C and the foaming pressure of 15 MPa. A possible reason for the result is that the foaming temperature of 179°C may be not in the PP foaming temperature window because PP, as a semicrystalline polymer, has a very narrow foaming temperature window. Increasing the pressure to 19 MPa resulted in the formation of a few isolated cells, which were very small. A possible explanation is that exposing the sample to CO_2 with a higher pressure is equivalent to an increase in the initial CO_2 concentration dissolved in the sample. However, the cell could almost not grow because of the lower foaming temperature and thus higher viscosity of

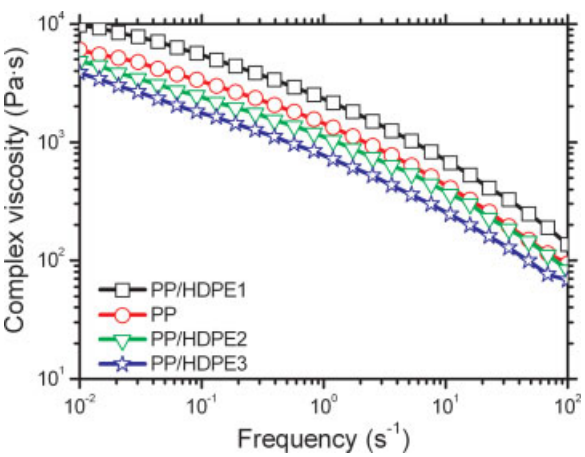

Figure 4 Complex viscosity versus the frequency for PP and PP/HDPE blends. [Color figure can be viewed in the online issue, which is available at www.interscience.wiley.com.]

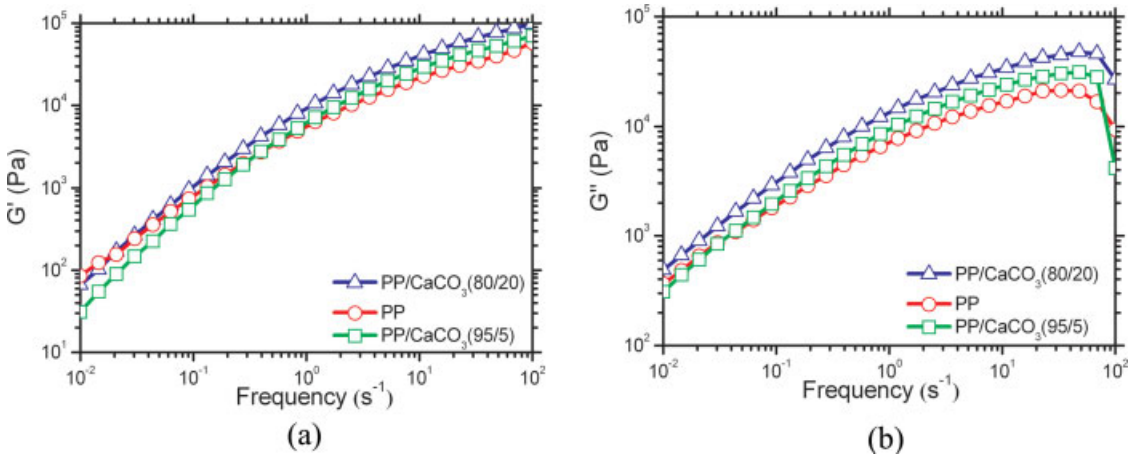

Figure 5 Experimental data for the storage and loss moduli (G' and G'') for PP and PP/nano-$CaCO_3$ composites at 179°C. [Color figure can be viewed in the online issue, which is available at www.interscience.wiley.com.]

PP. At the foaming pressure of 15 MPa, increasing the foaming temperature to 182°C led to the formation of many cells, which were mostly ellipsoidal. However, a clear nonuniformity of the cell diameter distribution was observed. This may be briefly explained as follows. First, the foaming temperature, 182°C, may be in the PP foaming temperature window. Second, the material became soft with increasing temperature, and thus a bubble was favored to grow. When a bubble grew in the polymer matrix, the polymer between the bubbles was stretched. Therefore, some individual cells coalesced into larger cells under the stretching force imposed onto the cell wall during the bubble growth.

Illustrated in Figure 8 are the cellular structures of foamed PP/HDPE blends at the foaming temperature of 179°C and the foaming pressures of 15 and 19 MPa. In comparison with pure PP, the incorporation of a minor phase of HDPE into the PP matrix improved the cellular structures of the foamed samples. The improved microcellular foamability of the PP/HDPE blends can be explained as follows. Poorly bonded interfaces are developed in the blending of immiscible PP and HDPE. The interfaces have much lower activation energy for bubble nucleation and so provide favorable heterogeneous nucleating sites for bubble formation.[6] The resulting microcellular foam structure is determined mainly by the number of nuclei, so the microcellular structure can be obtained from blends. Moreover, the cellular structures of the foamed blends are also related to the resulting morphology by blending. The melt shear viscosity ratio of the dispersed phase to the continuous phase in the blend is an important factor affecting the blend morphology. A higher viscosity ratio results in dispersed phase droplets of a larger size.[13–16] As previously mentioned, the three PP/HDPE blends used in this work had different viscosity ratios and so exhibited different morphologies.

Figure 8 shows that both the viscosities and storage moduli of the blends and the foaming pressure had significant effects on the cell structures of the foamed blends. At a foaming pressure of 15 MPa, uniformly distributed and well-developed microcellular structures were formed in both PP/HDPE1 and PP/HDPE2 blends, especially for the latter, the cells of which were very fine and uniform. This can be briefly explained as follows. The cell diameter of foams is controlled by the growth of cells and their coalescence, which are strongly affected by the storage modulus of the material during the foaming process. Both PP/HDPE1 and PP/HDPE2 blends exhibited higher storage moduli than pure PP at a very low frequency, as shown in Figure 3(a), which

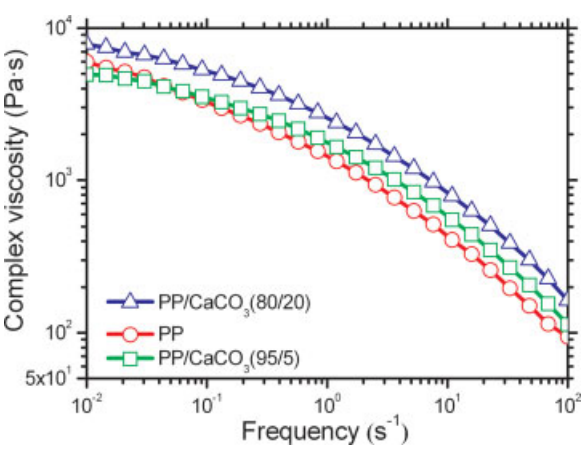

Figure 6 Complex viscosity versus the frequency for PP and PP/nano-$CaCO_3$ composites at 179°C. [Color figure can be viewed in the online issue, which is available at www.interscience.wiley.com.]

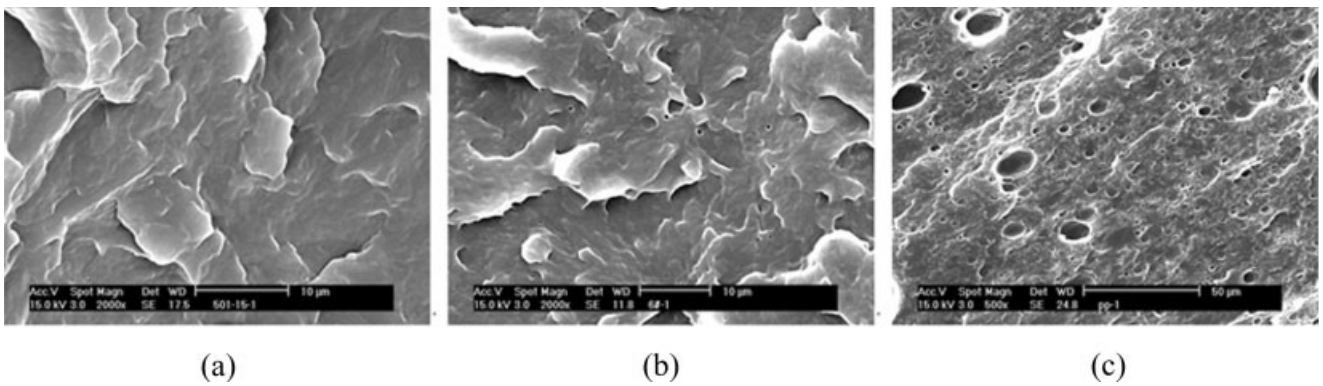

Figure 7 SEM micrographs of foamed PP at foaming pressures and temperatures of (a) 15 MPa and 179°C, (b) 19 MPa and 179°C, and (c) 15 MPa and 182°C.

may have inhibited the growth of cells and their coalescence, leading to a significantly small cell diameter. However, cell coalescence and collapse appeared in the foamed PP/HDPE3 blend. Moreover, its foam structure was not very uniform. This is because the PP/HDPE3 blend had the lowest viscosities and storage modulus (as shown in Figs. 2–4), and so it was difficult to maintain the microcellular structure.

On the whole, increasing the foaming pressure to 19 MPa resulted in larger bubbles and bubble coalescence and collapse, as shown in Figure 8(2). This may be explained as follows. As mentioned previously, exposing the sample to higher pressure CO_2 is equivalent to increasing the initial dissolved gas concentration in the sample, which results in the cell diameter becoming smaller and the number of cells becoming larger at the cell nucleation. However, a higher initial CO_2 concentration may lead to bubble coalescence during the bubble growth and eventually makes bubbles larger. As shown in Figure 8(a-2), a fully grown cell structure was developed in the foamed PP/HDPE1 blend because the PP/HDPE1 blend had the highest viscosities and storage modulus (as shown in Figs. 2–4) of all three blends and so the microcellular structure could be maintained. The most obvious bubble coalescence and collapse appeared in the foamed PP/HDPE3 blend, again because of its lowest viscosities and storage modulus.

Figure 9 illustrates the SEM micrographs of foamed PP/nano-$CaCO_3$ composites with different contents of nano-$CaCO_3$. In comparison with pure PP, adding the nano-$CaCO_3$ particles made PP easy to foam because nano-$CaCO_3$ particles play the role of a nucleating agent. More importantly, in the

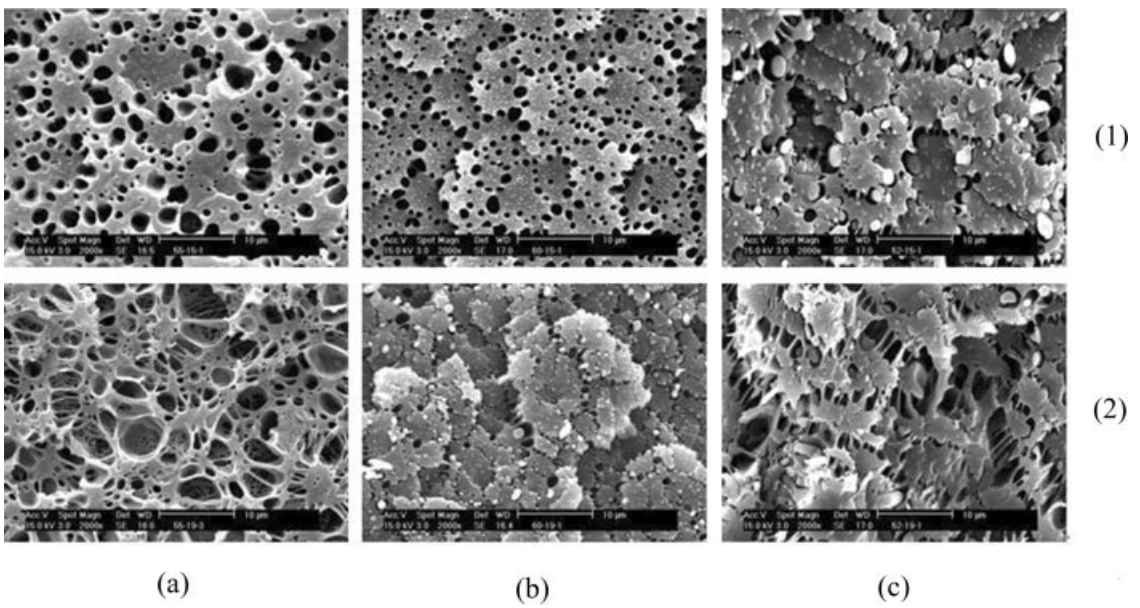

Figure 8 SEM micrographs of foamed (a) PP/HDPE1, (b) PP/HDPE2, and (c) PP/HDPE3 blends at foaming pressures of (1) 15 and (2) 19 MPa and a foaming temperature of 179°C.

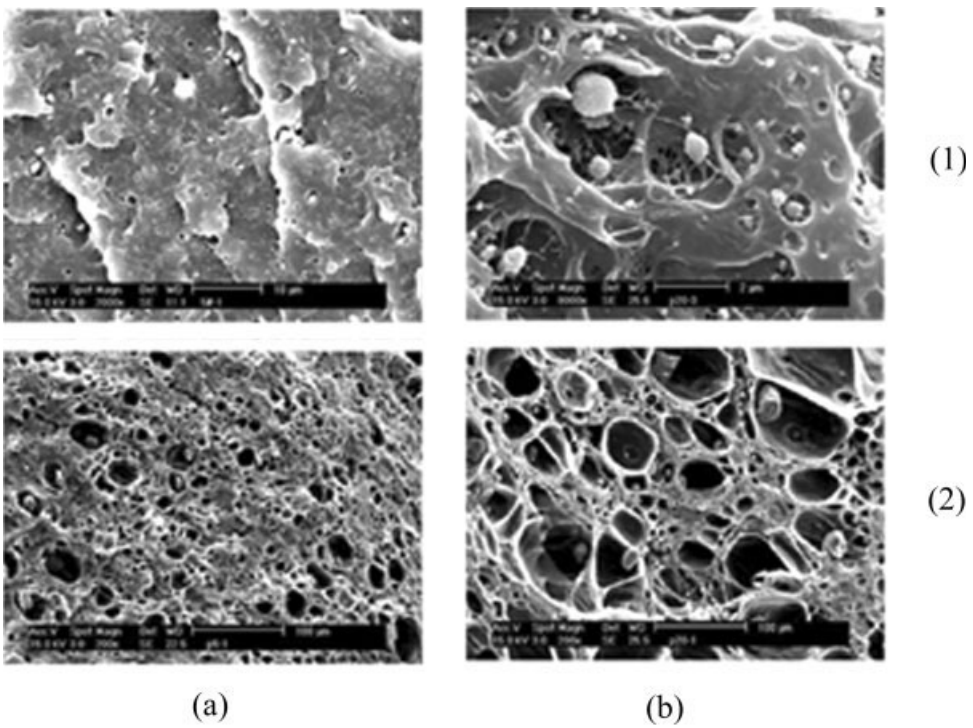

Figure 9 SEM micrographs of foamed (a) PP/nano-$CaCO_3$ (95/5 w/w) and (b) PP/nano-$CaCO_3$ (80/20 w/w) composites at foaming temperatures of (1) 179 and (2) 182°C and a foaming pressure of 15 MPa.

heterogeneous nucleation process containing nano-$CaCO_3$ particles, cell nucleation took place at the boundary between the matrix polymer and the dispersed nano-$CaCO_3$ particles. Recent work carried out by Huang et al.[17] demonstrated that for a PP/nano-$CaCO_3$ composite containing a lower loading (5 wt %) of nano-$CaCO_3$, the particles were finely dispersed in the PP matrix, and this provided much more effective nucleation sites during foaming. As a result, a cellular structure with very small cell sizes was achieved for the PP/nano-$CaCO_3$ (95/5 w/w) composite, as shown in Figure 9(a-1). When the nano-$CaCO_3$ concentration was increased to 20 wt %, the cellular structure of the foamed PP/nano-$CaCO_3$ composite exhibited a nonuniform distribution, as shown in Figure 9(b). This is because most particles coalesced at a higher nano-$CaCO_3$ content.[17] The coalesced $CaCO_3$ particles with large diameters made the bubbles around them have larger diameters, and finely dispersed particles with smaller diameters made the bubbles have smaller diameters.

PP/nano-$CaCO_3$ composites had lower storage moduli than PP at low frequencies, as shown in Figure 5(a). The lower storage modulus of the material made the nucleation easier but made the gas difficult to be held during the foaming process. As a result, nucleated cells were easier to rip or coalesce. This may be another probable reason for the nonuniform cellular structures, some spherical and some ellipsoidal, that formed in the foamed PP/nano-$CaCO_3$ composites.

Comparing Figure 9(1,2), we found that for both foamed PP/nano-$CaCO_3$ composites, the cells that formed at the foaming temperature of 182°C had a larger diameter than those at 179°C. This may be attributed to the fact that a higher foaming temperature made the material softer and the cells easier to grow in the PP matrix.

The cellular structure of the foamed PP/HDPE1/nano-$CaCO_3$ composite is illustrated in Figure 10.

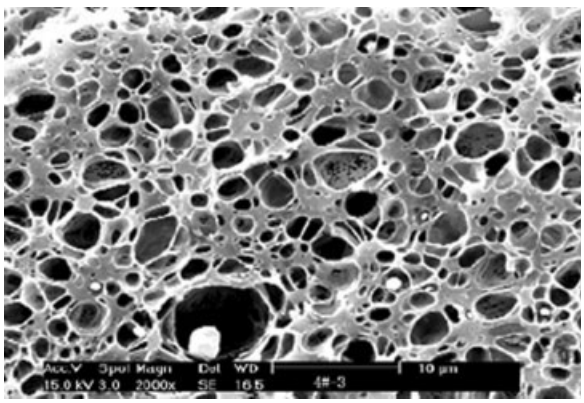

Figure 10 SEM micrograph of a foamed PP/HDPE1/nano-$CaCO_3$ (75/20/5 w/w/w) composite at a foaming temperature of 179°C and a foaming pressure of 15 MPa.

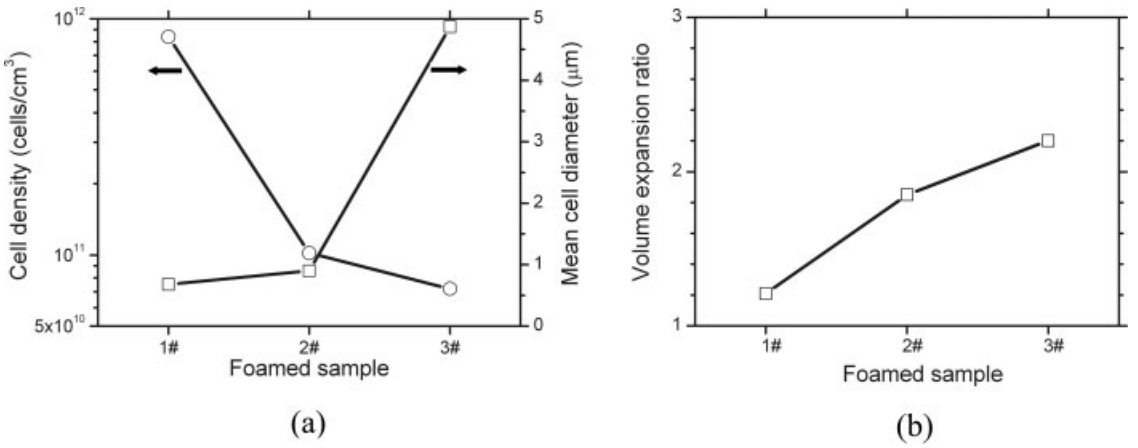

Figure 11 (a) Cell density and mean cell diameter and (b) volume expansion ratio for three foamed samples at a foaming temperature of 179°C and a foaming pressure of 15 MPa: ($1^{\#}$) PP/nano-$CaCO_3$ (95/5 w/w) composite, ($2^{\#}$) PP/HDPE1 blend, and ($3^{\#}$) PP/HDPE1/nano-$CaCO_3$ composite.

The nano-$CaCO_3$ particles played the role of a nucleating agent, and some cells grew around the nano-$CaCO_3$ particles.

Morphological parameters of the foamed samples

The morphological parameters of some foams were calculated from the SEM micrographs of foamed samples with eqs. (1) and (2), and their volume expansion ratio was calculated with eq. (3). The mean cell diameters, cell densities, and volume expansion ratios of the foamed PP samples through the incorporation of 5 wt % nano-$CaCO_3$, through blending with HDPE1, and through both blending with HDPE1 and the incorporation of 5 wt % nano-$CaCO_3$ are compared in Figure 11. All three samples were foamed at 179°C and 15 MPa. The foamed PP/nano-$CaCO_3$ (95/5 w/w) composite (sample 1) exhibited the largest cell density (8.4×10^{11} cells/cm^3) and the smallest volume expansion ratio of the three foamed samples. This is because a great deal of finely dispersed nano-$CaCO_3$ particles could improve the nucleation during the foaming process, but the higher viscosity of the PP matrix at 179°C retarded the cell growth. The cell density of the foamed PP/HDPE1/nano-$CaCO_3$ composite (sample 3) was smaller than that of the foamed PP/HDPE1 blend (sample 2).

The foamed PP/HDPE2 blend at 15 MPa and 179°C, the cell structure of which is shown in Figure 8(b-1), had a mean cell diameter of 0.7 μm and a cell density of 1.17×10^{11} cells/cm^3, which were the minimum and maximum, respectively, among the three foamed blends. This may be attributed to the fact that the shear viscosity ratio of the PP/HDPE2 blend was closer to unity (as shown in Fig. 2). Previous studies, such as ref. 18, demonstrated that the smallest dispersed phase domains in polymer blends are obtained when the viscosity ratio is close to unity. As mentioned previously, the interfaces that develop between PP and HDPE provide favorable heterogeneous nucleating sites for bubble formation. The smallest domains in the PP/HDPE2 blend provided more interfaces for nucleation. Therefore, it is worth studying the effect of the blend morphology on the cellular morphology of microcellular foaming.

CONCLUSIONS

PP, when it was blended with HDPE and/or nano-$CaCO_3$ particles were incorporated into it, exhibited greatly enhanced foamability compared with pure PP. HDPEs with higher viscosities and resulting blends with higher storage moduli were favorable for maintaining the microcellular structure. The blend with a viscosity ratio close to unity produced a microcellular foam with a very fine and uniform cell structure. Finely and uniformly dispersed nano-$CaCO_3$ particles in the PP matrix provided very effective nucleation sites and so produced a cellular structure with very small cell sizes. However, the large coalesced $CaCO_3$ particles made the cellular structure nonuniform. Moreover, adding nano-$CaCO_3$ to PP meant that the foaming could be performed at a lower foaming temperature in comparison with that for pure PP.

References

1. Okamoto, K. T. Microcellular Processing; Hanser: Munich, 2003.
2. Foam Extrusion: Principles and Practices; Lee, S. T., Ed.; CRC: Boca Raton, FL, 2000.
3. Colton, J. S. Mater Manufac Proc 1989, 4, 253.
4. Colton, J. S.; Suh, N. P. U.S. Pat. 5,160,674 (1992).
5. Doroudiani, S.; Park, C. B.; Kortschot, M. T. Polym Eng Sci 1996, 36, 2645.

6. Doroudiani, S.; Park, C. B.; Kortschot, M. T. Polym Eng Sci 1998, 38, 1205.
7. Rachtanapun, P.; Selke, S. E. M.; Matuana, L. M. J Appl Polym Sci 2003, 88, 2842.
8. Rachtanapun, P.; Selke, S. E. M.; Matuana, L. M. J Appl Polym Sci 2004, 93, 364.
9. Okamoto, M.; Nam, P. H.; Maiti, P.; Kotaka, T.; Nakayama, T.; Takada, M.; Ohshima, M.; Usuki, A.; Hasegawa, N.; Okamoto, H. Nano Lett 2001, 1, 503.
10. Nam, P. H.; Maiti, P.; Okamoto, M.; Kotaka, T.; Nakayama, T.; Takada, M.; Ohshima, M.; Usuki, A.; Hasegawa, N.; Okamoto, H. Polym Eng Sci 2002, 42, 1907.
11. Taki, K.; Yanagimoto, T.; Funami, E.; Ohshima, M. Polym Eng Sci 2004, 44, 1004.
12. Huang, H. X.; Wang, J. K. Proc ASME Mater Div 2005, 100, 575.
13. Potente, H.; Krawinkel, S.; Bastian, M.; Stephan, M.; Pötschke, P. J Appl Polym Sci 2001, 82, 1986.
14. Huang, H. X.; Huang, Y. F.; Yang, S. L. Polym Int 2005, 54, 65.
15. Huang, H. X. J Mater Sci 2005, 40, 1777.
16. Huang, H. X.; Huang, Y. F.; Li, X. J. Polym Test, to appear.
17. Huang, H. X.; Jiang, G.; Mao, S. Q. J Mater Sci 2006, 41, 4985.
18. Yang, K. M.; Lee, S. H.; Oh, J. M. Polym Eng Sci 1999, 39, 1667.